

Supplementary Material (ESI) for CrystEngComm

Supplementary Data for

Electronic and structural characterisation of a tetrathiafulvalene tetrathiafulvalene compound as potential candidate for ambipolar transport properties

*Francisco Otón,¹ Raphael Pfattner,¹ Egon Pavlica,² Yoann Olivier,³ Guido Bratina,² Jerome Cornill,³ Joaquim Puigdollers,⁴ Ramón Alcubilla,⁴ Xavier Fontrodona,⁵ Marta Mas-Torrent,*¹ Jaume Veciana¹ and Concepció Rovira.*¹*

-
1. Institut de Ciència de Materials de Barcelona (ICMAB-CSIC) and Networking Research Center on Bioengineering, Biomaterials and Nanomedicine (CIBER-BBN). Campus de la Universitat Autònoma de Barcelona, Bellaterra E-08193 (Barcelona) Spain. Fax: (+34) 935805729.
 2. Laboratory for Organic Matter Physics, University of Nova Gorica, Vipavska 13, SI-5000 Nova Gorica, Slovenia.
 3. Laboratory for Chemistry of Novel Materials. University of Mons, Place du Parc 20, B-7000 Mons.
 4. Dept Eng. Electrònica and CrNE. Universitat Politècnica Catalunya. E-08034 (Barcelona) Spain.
 5. Serveis Tècnics de Recerca. Universitat de Girona. Edifici Jaume Casademont (porta E), Pic de Peguera, 15.(La Creueta). E- 17003 Girona (Spain).

*Authors to whom correspondence should be addressed. E-mail: mmas@icmab.es; cun@icmab.es;

Table of Contents

Experimental details.

Figure S1. Cyclic voltammetry and Square Wave Voltammetry of compounds in *o*-dichlorobenzene at $t = 120^{\circ}\text{C}$ ($c = 10^{-3}$ M) using TBAHP ($c = 0.15$ M) as supporting electrolyte.

Figure S2. UV-vis spectra in *o*-dichlorobenzene at $t = 80^{\circ}\text{C}$ ($c = 1 \times 10^{-4}$ M).

Table S1. Crystal Data and Refinement Details for 1,4-naphthoquinone[2,3-*b*]tetrathiafulvalene.

Figure S3. Optical microscope image ($P=A=0$) of a typical single crystal OFET with graphite based source and drain electrodes in a Si/SiO₂ substrate.

Figure S4. Thermal evaporation process of BNQ-TTF thin films.

Figure S5. (Left) SEM image of an evaporated thin films. (Right) XRD of the same film. Peaks in the box correspond to the 0,0,*x* plane on the crystal cell.

Figure S6. Output I-V curve of a typical thin film based OFET with Al based source and drain electrodes.

Figure S7. AFM images of BNQ-TTF layer in thin-film transistor.

Figure S8. Transfer characteristics of a BNQ-TTF thin film OFET with Al top-contact source and drain electrodes. Semilogarithmic plot of a p-type(left) and n-type(right) saturation transconductance as a function of ($V_{\text{SG}} - V_{\text{th}}$), the threshold voltage corrected gate voltage.

References

S5

S6

S6

S7

S7

S8

S8

S8

S9

S9

S2

Experimental details.

Materials and Methods. All reactions were carried out under Ar using solvents which were dried following routine procedures. Graphite paste XC-12 was purchased from Dotite and thermally grown silicon dioxide was purchased from Si-Mat. Chemical reagents obtained from commercial sources were used without further purification. Column chromatography was performed using silica gel (60 A C.C. 35-70 μm , sds) as the stationary phase. The MALDI-TOF MS spectra were recorded on a Bruker Ultraflex II TOF spectrometer. Infrared spectra were recorded on a Perkin-Elmer FT-IR Spectrum One spectrometer. UV-Vis spectra were performed in *o*-dichlorobenzene heated at 80 °C ($c = 1 \times 10^{-4}$ M) using a VARIAN CARY 5000 spectrophotometer. Elemental analyses were carried out on a Carlo Erba CE 1108 Elemental Analyser. Cyclic voltammograms (CV) were performed with a conventional three-electrode configuration consisting of platinum wires as working and auxiliary electrodes and Ag/AgCl as reference electrode. These experiments were carried out in a 10^{-3} M solution of the corresponding TTF derivative in *o*-dichlorobenzene, thermostated at 120 °C to be able to solubilise the materials, and containing 0.1 M of (*n*-C₄H₉)₄PF₆ (TBAHP) as supporting electrolyte. Deoxygenation of the solutions was performed previously to the experiments by bubbling nitrogen for at least 10 min, and the working electrode was cleaned after each run. The CVs were recorded with an increasing scan rate from 0.05 to 0.50 Vs⁻¹. Ferrocene was used as an internal reference both for potential calibration and for reversibility criteria. All of the potential values reported are relative to the Fc⁺/Fc couple at room temperature. Under these conditions ferrocene has a redox potential of $E^0 = 0.440$ V vs Ag/AgCl sat. electrode and the anodic-cathodic peak separation is 67 mV. Crystallographic data of **1** and **3** were measured in a Bruker SMART Apex CCD using graphite-monochromated Mo K α radiation ($\lambda = 0.71073$ Å) from an X-Ray Tube. The measurements were made in the range 2.60 to 28.18° for θ . Full-sphere data collection was carried out with φ and ω scans. Programs used: data collection, Smart version 5.631 (Bruker AXS 1997-02); data reduction, Saint + version 6.36A (Bruker AXS 2001); absorption correction, SADABS version 2.10 (Bruker AXS 2001). Structure solution and refinement was done by using SHELXTL Version 6.14 (Bruker AXS 2000-2003). The structure was solved by direct methods and refined by full-matrix least-squares methods on F². The

non-hydrogen atoms were refined anisotropically. The H-atoms were placed in geometrically optimized positions and forced to ride on the atom to which they are attached. Single crystal OFETs were fabricated on 200 nm thermally oxidized silicon substrates. Crystals were formed on the substrate by drop casting a solution of 0.5- 1.0 mg of the compounds in 1 ml of toluene or chlorobenzene and allowing the solvent to evaporate slowly under darkness and reduced ambient humidity. The prepared devices were measured in a Süss Microtech Probe Station EP4 equipped with micromanipulators and with a two-channel Keithley SourceMeter 2612. Graphite paste used as source and drain electrodes was applied on the mounted crystals with a small brush and dried in air. Thin film OFETs were prepared and characterized under nitrogen atmosphere. Organic layers were deposited by spin coating onto p⁺⁺ Si(001) substrates, covered by 200 nm-thick thermally grown oxide layer and a 100 nm-thick spin-coated polystyrene film from 2 %wt toluene solution. Spin coating was performed at 3000 rpm for 70 s with 500 rpm/s acceleration. The samples were annealed at 100°C for 3 h in order to remove the remaining solvent. Subsequently, the substrates were transferred into the evaporation chamber, without exiting the nitrogen atmosphere. BNQ-TTF thin films were thermally evaporated onto the substrates at room temperature, and at a base pressure of 10⁻⁶ mbar. The growth rate was 0.2 nm/min. Nominal thickness of the BNQ-TTF layers, as determined during evaporation by the quartz thickness monitor was 60 nm. Subsequently, 60 nm-thick Al top-contact drain and source electrodes were evaporated through a shadow mask. Current-voltage measurements of the resulting devices was performed with Keithley SourceMeter 2400 and Picoammeter 6487 in dark and under nitrogen atmosphere.

Computational Details: Quantum chemical calculations: Geometries were fully optimized with tight convergence criteria at the Density Functional Theory (DFT) level with the Gaussian 09 package (A02 release),¹ using the B3LYP² functional and the 6-31G(d,p) basis set. All energies are not corrected for the zero-point vibrational energy. The electronic structures and the reorganization energies were calculated at the same level of theory. Transfer integrals have been calculated at the DFT level with the B3LYP functional and TZP basis set, using the fragment approach implemented in the ADF package with the

methodology described in Ref^{3, 4}. Internal reorganization energies were calculated with the B3LYP functional and 6-31G(d,p) basis set.

Computational Details: Kinetic Monte Carlo: The calculated Marcus transfer rates are injected into a Kinetic Monte-Carlo (KMC) algorithm in order to propagate a charge in the system and estimate the hole mobility. In our KMC scheme, detailed in [Olivier06], the charge is initially localized on a given molecule i and hops to the molecule j , chosen on the basis of the transfer probability expressed as:

$$P_{ij} = \frac{k_{ij}}{\sum_l k_{il}} \quad (3)$$

where k_{ij} is the transfer rate (corresponding to the inverse of the hopping time) between molecule i and j calculated with equation (1) and the sum index l runs over all possible neighbors of molecule i . After n hopping events, the mobility is calculated as:

$$\mu_n = \frac{d_n}{t_n \cdot F} \quad (4)$$

with d_n is the total distance traveled by the charge in the field direction during the simulation time t_n and F the norm of the electric field. A large number of hopping events (more than 10^{10} iterations) have been generated in order to get converged estimates of the mobility values, as supported by the standard deviation values.⁵

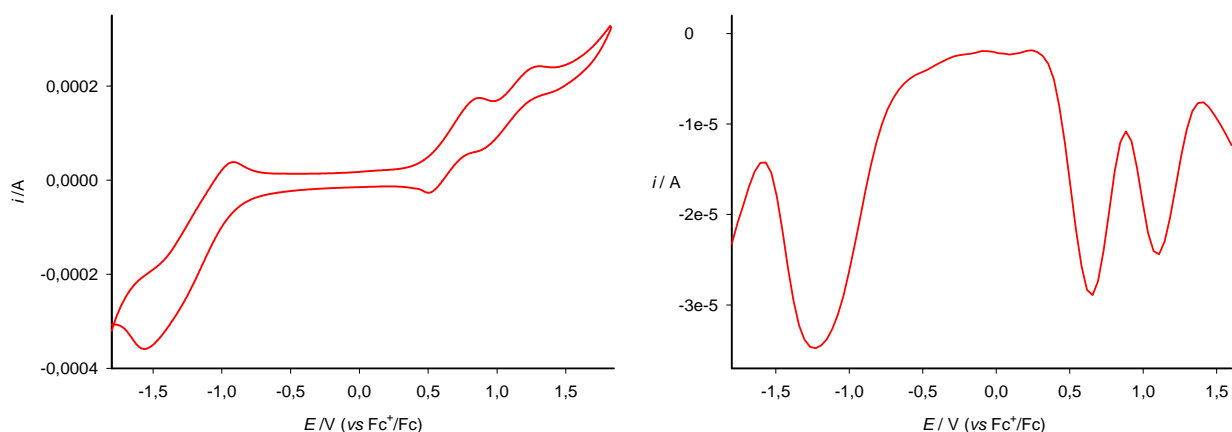


Figure S1. Cyclic voltammetry and Square Wave Voltammetry of BNQ-TTF in *o*-dichlorobenzene at $t = 120^\circ\text{C}$ ($c = 10^{-3}$ M) using TBAHP ($c = 0.15$ M) as supporting electrolyte.

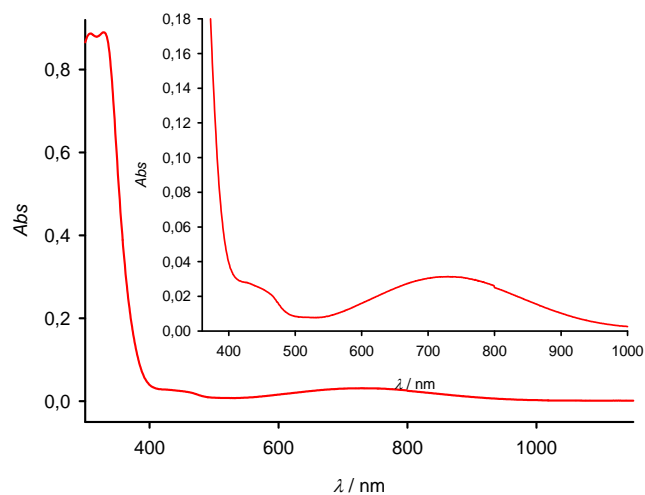


Figure S2. UV-vis spectra in o-dichlorobenzene at $t = 80^{\circ}\text{C}$ ($c = 1 \times 10^{-4}$ M).

Table S1. Crystal Data and Refinement Details for 1,4-naphthoquinone[2,3-b]tetrathiafulvalene. (CCDC 812334).

empirical formula	$\text{C}_{24}\text{H}_{18}\text{N}_2\text{O}_4\text{S}_4$
fw, g mol^{-1}	464.52
Method	Single-Crystal
λ , Å	Mo-K α , 0.71073
cryst syst	Monoclinic
SPGR, Z	$\text{P}2_1/\text{n}$, Z=2
a, Å	3.881(4)
b, Å	7.532(8)
c, Å	31.35(3)
α , °	90
β , °	90.590(18)
γ , °	90
V, Å ³	916.4(17)
ρ_{calc} , g cm^{-3}	1.683
T, K	300(2)
2θ range, °	4.04-55.12
R1, wR2	0.2976, 0.4364

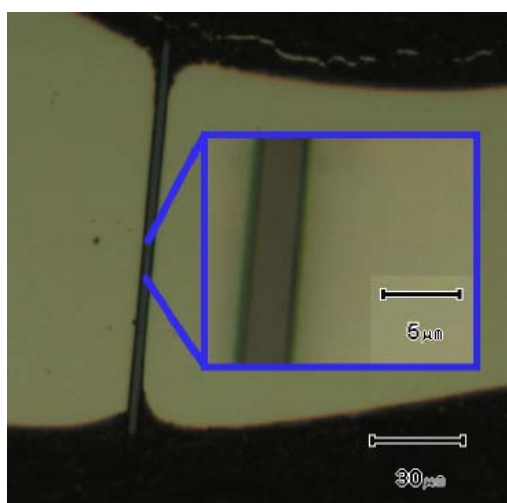


Figure S3. Optical microscope image ($\Phi_{P/A}=0^\circ$) of a typical single crystal OFET with graphite based source and drain electrodes in a Si/SiO₂ substrate.

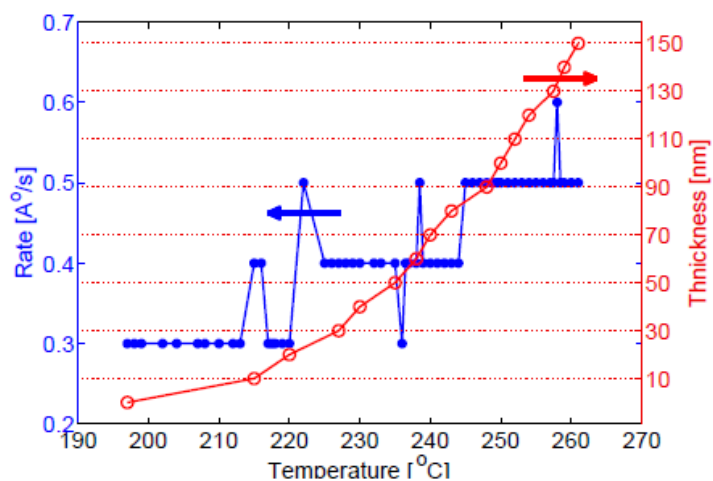


Figure S4. Thermal evaporation process of BNQ-TTF thin films.

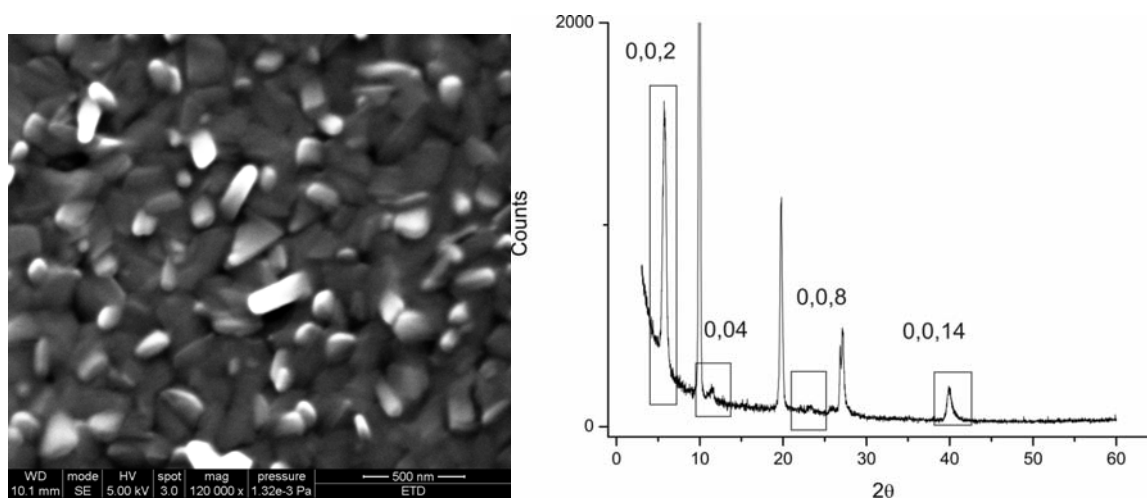


Figure S5. (Left) SEM image of an evaporated thin films. (Right) XRD of the same film. Peaks in the box correspond to the 0,0,x plane of the crystal cell.

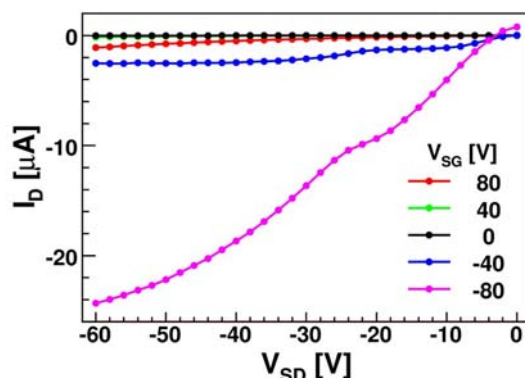


Figure S6. Output I-V curve of a BNQ-TTF based thin-film OFET with Al based source and drain electrodes.

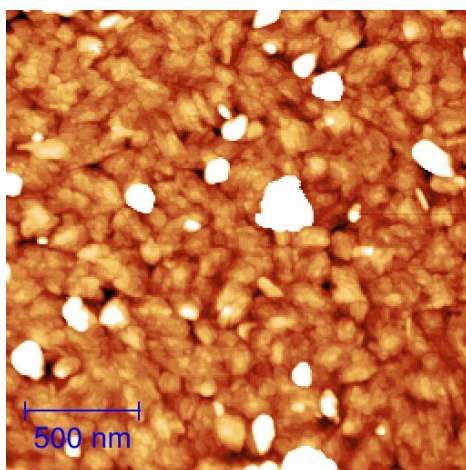


Figure S7. AFM image of a BNQ-TTF layer inside a thin-film OFET channel. The scan size of the image is $2\mu\text{m}$. The vertical scale of the image is 15nm. The thickness of BNQ-TTF layer is 60 nm. The BNQ-TTF forms a layer of interconnected grains, with a diameter of approximately 100 nm and RMS roughness of 1.8 nm. Columnar structures extend out of the plane of the film. The surface density of these columns is approximately $10/\mu\text{m}^2$. The maximum observed height of the columns above the mean surface of the organic layer is 120 nm.

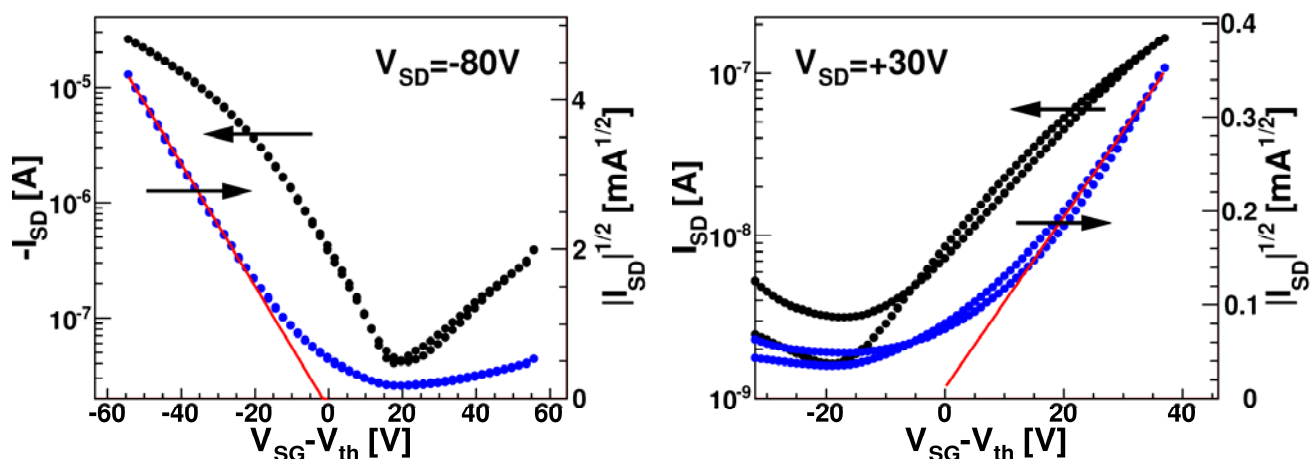


Figure S8. Transfer characteristics of a BNQ-TTF thin film OFET with Al top-contact source and drain electrodes. Figures present semilogarithmic plot of a p-type(left) and n-type(right) saturation transconductance as a function of $(V_{SG} - V_{th})$, the threshold voltage corrected gate voltage. The solid lines are used to estimate the field-effect mobility for the p-type and n-type charge carriers, respectively.

References.

1. G. 03, Revision, C01, M. J. Frisch, G. W. Trucks, H. B. Schlegel, G. E. Scuseria, M. A. Robb, J. R. Cheeseman, J. Montgomery, J. A., T. Vreven, K. N. Kudin, J. C. Burant, J. M. Millam, S. S. Iyengar, J. Tomasi, V. Barone, B. Mennucci, M. Cossi, G. Scalmani, N. Rega, G. A. Petersson, H. Nakatsuji, M. Hada, M. Ehara, K. Toyota, R. Fukuda, J. Hasegawa, M. Ishida, T. Nakajima, Y. Honda, O. Kitao, H. Nakai, M. Klene, X. Li, J. E. Knox, H. P. Hratchian, J. B. Cross, V. Bakken, C. Adamo, J. Jaramillo, R. Gomperts, R. E. Stratmann, O. Yazyev, A. J. Austin, R. Cammi, C. Pomelli, J. W. Ochterski, P. Y. Ayala, K. Morokuma, G. A. Voth, P. Salvador, J. J. Dannenberg, V. G. Zakrzewski, S. Dapprich, A. D. Daniels, M. C. Strain, O. Farkas, D. K. Malick, A. D. Rabuck, K. Raghavachari, J. B. Foresman, J. V. Ortiz, Q. Cui, A. G. Baboul, S. Clifford, J. Cioslowski, B. B. Stefanov, G. Liu, A. Liashenko, P. Piskorz, I. Komaromi, R. L. Martin, D. J. Fox, T. Keith, M. A. Al-Laham, C. Y. Peng, A. Nanayakkara, M. Challacombe, P. M. W. Gill, B. Johnson, W. Chen, M. W. Wong, C. Gonzalez and J. A. Pople, Gaussian, Inc., Wallingford CT, 2004.
2. L. J. Bartolotti and K. Fluchick, *Reviews in Computational Chemistry*, VCH, New York, 1996.
3. E. F. Valeev, V. Coropceanu, D. A. d. Silva, S. Salman and J.-L. Brédas, *J. Am. Chem. Soc.*, 2006, **128**, 9882-9886.
4. K. Senthilkumar, F. C. Grozema, F. M. Bickelhaupt and L. D. A. Siebbeles, *J. Chem. Phys.*, 2003, **119**, 9809-9817.
5. Y. Olivier, V. Lemaire, J.-L. Brédas and J. Cornil, *J. Phys. Chem. A*, 2006, **110**, 6356-6364.